Proceedings of the ASME 2020
Turbomachinery Technical Conference and Exposition
GT2020
June 22-26, 2020, London, England

GT2020-14511

QUANTIFICATION OF VARIATION IN COMBUSTION INSTABILITY AMPLITUDE IN A MULTI-NOZZLE CAN COMBUSTOR

Seth Westfall, Olivia Sekulich, Wyatt Culler, Stephen Peluso, Jacqueline O'Connor
The Pennsylvania State University, University Park, PA, USA

ABSTRACT

In this work, we quantify the level of variation in unstable combustion oscillation amplitudes and identify the source of this variation in a multi-nozzle can combustor. At conditions where pollutant emissions are reduced, lean-premixed combustors can undergo thermoacoustic instability when pressure and heat release rate oscillations couple. A commonly used method for suppressing instability is fuel staging, which is a method where fuel is unevenly distributed between nozzles in a multi-nozzle combustor. Our work follows others who have characterized the effect of fuel staging on combustion instability and the mechanisms by which it works during both steady-state and transient operation. One of the outcomes from our previous work was that certain instability operating points display a high level of pressure oscillation amplitude variation. Instead of oscillating at a constant limit-cycle amplitude, the pressure oscillation amplitude varies significantly in time. In this work, we use the concept of permutation entropy to quantify the level of variation in the pressure fluctuation amplitude. We correlate the level of variation with a number of state variables over a range of operating conditions, 291 test cases in all. These state variables include mixture equivalence ratio; transient timescale, amplitude, and direction; hardware temperatures; gas temperatures; and thermoacoustic damping and growth rates. Significant pressure oscillation amplitude variation occurs when the thermoacoustic damping rate is low. The damping and growth rates can be low for a number of reasons, but they are highly correlated with the metal temperature of the centerbody, where the flames are anchored; lower temperatures result in lower damping rates during stable operation and lower growth rates during unstable operation. These results show the importance of the thermal boundary condition on the time-dependent behavior of the thermoacoustic instability.

NOMENCLATURE

A_i	Harmonic Amplitude
H_n	Permutation Entropy
h_n	Normalized Permutation Entropy
n	Permutation Order
p_k	Relative frequency of symbolic pattern
t	Time
v_n	Growth Rate
v_i	Damping Rate
β	Flame driving energy
τ_{pe}	Permutation Entropy Time Lag
$\tau_{transient}$	Fuel Staging Timescale
ω_i	Frequency

INTRODUCTION

Modern power generation gas turbines meet NO_x emission requirements by employing lean-premixed combustion [1]. However, lean-premixed combustion is more susceptible to combustion instabilities that arise from coupling between combustor pressure fluctuations and flame heat release rate oscillations [2]. This coupling can drive the acoustic pressures to dangerously high oscillation levels, which, if left unchecked, can reduce the life of or destroy engine components.

There are several techniques to suppress combustion instabilities. Passive techniques, such as Helmholtz resonators and quarter-wave tubes, are preferred in industry due to their simplicity and durability [1]. Another common passive technique is fuel staging, where fuel is unevenly distributed in a multi-nozzle combustor to suppress instabilities by changing the local heat release rate [3]. Fuel staging has been successfully used in commercial hardware and recent work has identified a potential mechanism by which staging suppresses instabilities [4,5]. Samarasinghe et al. [4] hypothesized that fuel staging breaks the coupling mechanisms that cause combustion instabilities through phase cancellation. They used high-speed CH* chemiluminescence imaging and planar laser-induced fluorescence of OH (OH-PLIF) to show that when the inner and outer nozzles were equally fueled at a specific equivalence ratio, the heat release rate oscillations between nozzles were in phase. Then, with increased fuel staging, the combustor stabilized

because the staged and un-staged flames oscillated out of phase, resulting in a near-zero global heat release rate oscillation.

The current work is motivated by previous work on transient combustor operation, particularly the transition between stable and unstable states using fuel staging. Studies of transient behavior can be categorized into two types: one where the transient operation is commanded via a deliberate change in an operating parameter like equivalence ratio or fuel staging [4–8], and one where the combustor is operated very near a bifurcation point and the noise-driven transition from stable to unstable operation is observed [9–14]. The results from these two types of experiments can be significantly different, as the timescale over which transient operation is commanded has been shown by our group [15] and others [8] to impact the final state of the system. In an extreme case, appropriate application of timescale variation can result in what Bonciolini and Noiray refer to as a "bifurcation dodge" [15], a process that could not be achieved by operating the combustor at a single operating condition near the bifurcation point and allowing noise to drive the system.

Our previous work has focused on the first type of transient experiment, where variations in fuel staging are commanded with different transient directions, amplitudes, and timescales [4–7]. A few key learnings emerged from this previous work. First, combustion instability is stabilized through a phase-cancellation mechanism between nozzles [4]. Second, both central and outer nozzles can be used to suppress instability through fuel staging [6]. However, in our experimental facility, the center nozzle produced greater combustion stability because the damping rate of the system was higher [5]. Third, the characteristic rise time, or the time it takes to transition between stable and unstable operation, is longer than the characteristic decay time for all commanded transient time scales and staging equivalence ratios [6,7]. Lastly, the combustor damping rate is a strong function of staging equivalence ratio [6]. Combustor damping rate is one way to quantify the stability margin of the combustor, where a larger damping rate means a wider stability margin [16,17].

During our previous testing, we noted that roughly half of the test cases exhibit some level of variation in the amplitude of the pressure oscillations during instability. This variation is different than the intermittency observed as a route to instability, where others have identified this intermittency as variations in pressure oscillations between low-amplitude, aperiodic bursts and high-amplitude, periodic bursts [18,19]. Nair et al. [12] showed that intermittency is a dynamic state that can be a precursor to instability through phase-space reconstruction and recurrence plots. Furthermore, previous studies used phase-space trajectories [20], recurrence analysis [21], and bifurcation analysis [20], to suggest that intermittency can occur before and after combustion instabilities. Additionally, intermittency in bluff-body flames was seen to be a result of pattern formation, where the turbulent flow exhibits spatial and temporal patterns to self-organize [22]. In these cases, the inherent hydrodynamic instability characteristics of the combustor lead to large-scale vortex roll-up, which creates the pressure oscillations that cause intermittency that leads to instability.

One method to quantify variation in the pressure oscillation amplitude is permutation entropy, proposed by Bandt and Pompe [23], which was developed to analyze time-varying signals through symbolic dynamics and entropy concepts. Permutation entropy calculates the orderliness of a signal and assigns a larger value to those signals that have less order. Using permutation entropy to quantify variations in signals has a number of advantages, including its robustness against noise and low computational overhead [23]. Many fields such as medicine, physical systems, economics, and environmental studies have used permutation entropy for signal analysis [24].

Permutation entropy has been used in the combustion literature as an analytical tool to better differentiate between unstable and stable thermoacoustic oscillations. Sampath et al. [25] used permutation entropy to confirm that a lower equivalence ratio operating condition displayed higher intermittency. Murayama et al. [26] used permutation entropy, in conjunction with Jensen-Shannon statistical complexity, to decipher between periodic oscillations and noisy chaos. Additionally, Wabel et al. [27] showed that permutation entropy was a good instantaneous measure of combustion instability, as it was relatively immune to noise. However, they were not able to use permutation entropy to predict combustion instability onset, instead analyzing fuel line pressure changes using short-lag autocorrelation. The previous three studies utilized permutation entropy to identify the type of combustion instability, whereas we will use it as a way to quantify the level of variation in the instability amplitude.

The focus of the current study is to better understand the conditions under which variation in the combustion instability amplitude occurs in transient fuel staging studies. In particular, we are interested in what would cause the system to display higher levels of variation after one transient vs. another. This goal is achieved by analyzing a large number of test cases – 291 – and linking the operating parameters to combustion instability amplitude variation.

EXPERIMENTS AND METHODS

Experimental overview

All experimental data was taken in a multi-nozzle can combustor, detailed by Samarasinghe et al. [28] and shown in Figure 1. The five-nozzle combustor has one center nozzle that is surrounded by the other four nozzles every 90°. Based on our previous convention, the nozzles have been named Center (center nozzle), and Nozzles 1, 2, 3, and 4 (outer nozzles). The majority of the fuel is delivered upstream of a choke point and the fuel and air mixture is balanced using a series of perforated plates to ensure that the same flow rate enters each of the five nozzles. Fuel can also be directly injected in the nozzle, where it flows into the air stream through small holes on the upstream side of the swirler vanes. This secondary fuel injection location is used to add or subtract fuel during the transient fuel-staging tests. Table 1 lists critical test parameters used.

Operating conditions

In order to better understand variations in instability amplitude, we analyze a large number of tests where we varied the staging nozzle, staging equivalence ratio, transient direction, and transient duration. This combustion system displays a single, quarter-wave instability mode at unstaged equivalence ratios above ϕ=0.70 for the operating conditions of this study (summarized in Table 1). The instability frequency is 530 Hz and the signal to noise ratio of the instability is on the order of 100 for all cases, even when the amplitude of the instability varies in time. We follow previous definitions of unstable behavior from this experiment, where instability is defined as a tonal pressure oscillation with an amplitude greater than 0.5% of the mean pressure and a signal to noise ratio of at least 30 [4].

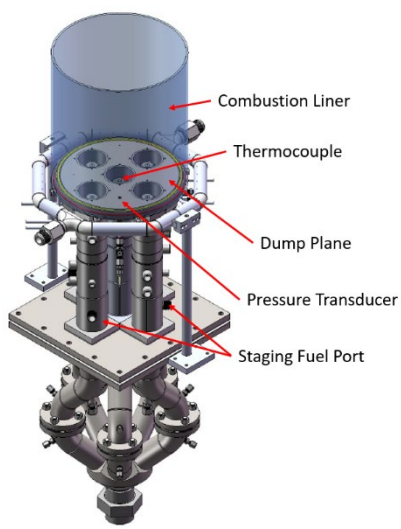

Figure 1. Multi-nozzle combustor experiment.

Table 1. Summary of experimental conditions

Parameter	Value
Inlet temperature	473 K
Nozzle bulk velocity	26 m/s
Inlet Reynolds number (Re_D)	17,000
Nozzle swirl number	0.7
Air mass flow rate	0.142 kg/s
Thermal power	291 kW

The nozzle through which staging fuel flowed was varied to test whether there was a systematic difference between symmetric and asymmetric fuel staging; it was found that there was no difference in instability suppression efficacy [7]. Staging equivalence ratio was studied by changing the staging nozzle's local equivalence ratio from ϕ=0.70 to either ϕ=0.80, 0.85, or 0.90 to control the instability [6,29]. The transient durations tested were 1 millisecond (ms), 16 ms, 4000 ms, and 10000 ms. The 1 and 16 ms durations are considered "short" durations because the fuel staging timescales are shorter than other timescales in the system, particularly heat transfer timescales. Previous work in this experiment [7] and in others [8,15] have shown that heat transfer is the critical timescale for comparison during transient operation in combustion systems; rough conjugate heat transfer calculations and results from work by Culler et al. [6] indicate that heat transfer timescales are on the order of seconds in this facility. The 4000 and 10000 ms transient durations are termed the "long" durations because the fuel staging is executed more slowly and the transient timescales are similar to the heat transfer time scales. Table 2 lists the test conditions included for analysis in the present study.

Table 2. Test matrix with transient timescale, staging equivalence ratio, staging nozzle, and the number of rise and decay tests at each staging condition.

$\tau_{Transient}$ (ms)	$\phi_{Staging}$	Staging Nozzle (Rise / Decay Test)
1	0.80	Center (13/15) Nozzle 2 (2/5) Nozzle 4 (1/0)
	0.85	Center (18/28) Nozzle 4 (2/8) Nozzle 2 (2/7) Nozzle 1 (3/6)
	0.90	Center (12/17) Nozzle 1 (5/7) Nozzle 4 (2/5) Nozzle 2 (3/4) Nozzle 3 (2/1)
16	0.80	Center (9/8)
	0.85	Center (7/7)
4000	0.80	Center (5/8)
	0.85	Center (6/11)
10000	0.80	Center (14/13)
	0.85	Center (15/16)
	0.90	Center (2/2)

The transient direction, called "rise" for transitions from stable to unstable conditions or "decay" for transitions from unstable to stable conditions, was studied to determine if combustion instability displayed hysteresis. Examples of these operating conditions are shown in Figure 2, where Figure 2(a) and (b) show decay cases and (c) shows a rise case.

Diagnostics

Experimental data was collected over 8 seconds for the short-timescale tests and 16 seconds for the long-timescale tests. For both rise and decay cases, fuel staging was actuated at 4 seconds to allow for stabilization of the steady-state condition both before and after the transient.

A pressure transducer (PCB 112A22), installed in the dump plane, was used to collect combustor pressure fluctuations at 16,384 Hz. The pressure data was high-pass filtered to reject frequencies below 10 Hz. Additionally, several K-type (Omega) thermocouples were installed in the test rig. We report the temperature from the thermocouple at the tip of the centerbody as it is closest to the flame anchoring point.

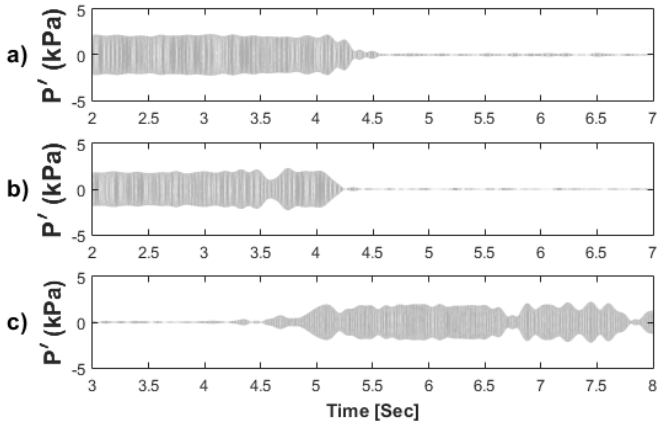

Figure 2. (a) Low apparent variation in a decay case, (b) medium apparent variation in a decay case, and (c) high apparent variation in a rise case.

Data analysis

Permutation entropy of the absolute value of the pressure time signal was calculated for each test case using the MATLAB function PETROPY written by Reidl et al. [24]; the permutation entropy calculation process is detailed in Appendix A. In all calculations, we normalize the permutation entropy for better comparison between cases. Careful consideration was given to the function's inputs as the results of the calculation depend greatly upon them; the inputs considered are the time signal (x_i), permutation order (n), and time lag (τ_{pe}). We use the absolute value of combustor pressure time signal to calculate the permutation entropy for two reasons. First, the absolute value better highlights the variations in the amplitude variation, making it easier for the algorithm to identify these amplitude variations. Second, the permutation entropy changes significantly between the unstable and stable parts of the signal when the absolute value is used, but less so when the original pressure time series is used. To understand the sensitivity of permutation entropy to the other input parameters, we performed two sensitivity studies.

Figure 3(a) shows the sensitivity of the permutation entropy calculation to different values of the permutation order for an instability decay case. Permutation orders were chosen based on suggestions by Riedl et al. [24], where previous studies on unsteady combustion have used permutation orders of 750 [27], 6 [30], and 5 [25]. We choose a permutation order of 5 because it followed similar analyses on combustion systems and it showed significant sensitivity to the time-varying amplitude of the pressure signal. Figure 3(b) shows the sensitivity of the calculation to the time lag, τ_{pe}. Small time lags were optimal for oscillations in the frequency range of the combustor instability (~530 Hz) and so the final time lag for the calculations is 6 Hz.

To capture the temporal variations in permutation entropy, we incorporated a "sliding window" over which to calculate permutation entropy, following the work of Wabel et al. [27] and Sampath et al. [25]. Data is analyzed in window sizes of 1 second centered a given time. Then the window is then shifted 0.05 seconds and permutation entropy is re-calculated for the next time, providing permutation entropy as a function of time, as in Figure 3.

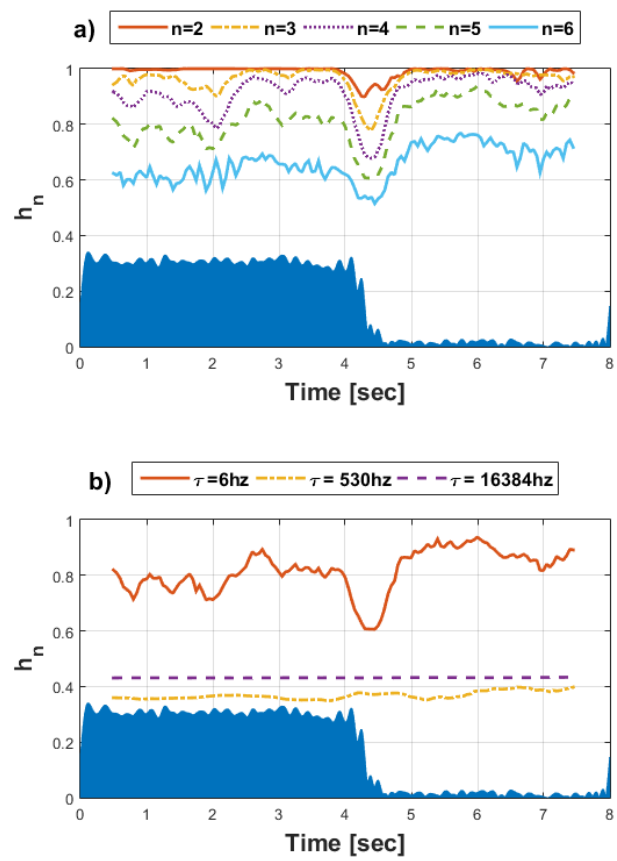

Figure 3. (a) Permutation order sensitivity plot for a typical decay case with τ_{pe} = 6 Hz. (b) Time lag sensitivity plot for the same decay case with n = 5. Absolute value of the acoustic pressure fluctuation is in blue.

Instability damping and growth rates are calculated to quantify the stability margin of the system, following the methods by Stadlmeier et al. [17]. In a thermoacoustic system, the damping and growth rate are the same quantity, but damping rate can only be calculated when the combustor is stable (or damped) and growth rate can only be calculated when the combustor is unstable. Given that we are interested in this quantity during both stable and unstable operation, we report both and use the two different names to identify the system stability at the time that the quantity was calculated.

Combustor damping rate is calculated following the method by Stadlmeier et al. [17] and used previously in our group by Culler et al. [6]; it is calculated for stable portions of the signal. The damping rate, υ_i, is calculated using the pressure auto-correlation function in Eq. 1. Bayesian network modeling, which uses Markov Chain Monte Carlo methods to simulate probability densities of the parameters in Eq. 1, is used with a Gibbs sampler (JAGS [31]) to find the best fit for the damping rate, υ_i, the initial

amplitude, A, and the frequency, ω, where t is the time delay in the autocorrelation calculation.

$$k_{p'p'} = \sum_{i=1}^{I} exp(-v_i t) A_i \, cos(\omega_i t) \qquad (1)$$

A similar method is used for calculating the instability growth rate, which follows the method of Hummel et al. [32] and is calculated for unstable sections of the pressure signals. Here, the auto-correlation of the unstable pressure envelop, as in Eq. 2, is fit using the Bayesian network to calculate the growth rate, v_n. The pressure envelop is determined using the Hilbert transform, as described in our previous work by Culler et al. [6].

$$k_{GG} = exp(-2v_n t) \qquad (2)$$

RESULTS AND DISCUSSION

In all, 291 test cases taken over a span of three years were analyzed to understand the reasons behind variation in the combustion instability amplitude. We hypothesize that the variation is connected to the thermoacoustic damping and growth rates of the system, where higher variation of the instability amplitude is the result of a lower growth rate in the system. To test this hypothesis, we first connect variation levels to damping and growth rates, then understand the reasons why the damping or growth rate of the system may vary at different operating conditions.

Figure 4 shows a scatter plot of all 291 cases comparing the root-mean-square (RMS) permutation entropy against the RMS combustor pressure during unstable operation. The RMS of the permutation entropy is used as a metric for amplitude variation over the entire time signal rather than the mean as it is more indicative of temporal variations in the signal when the normalized permutation entropy is calculated with a short time lag, as was done here. Figure 4 shows that RMS permutation entropy is not correlated to the strength of the acoustic oscillation and, as such, is not a good indicator of when the combustor is unstable. Instead, as we show next, it is a good indicator of the variation of the pressure oscillation amplitude.

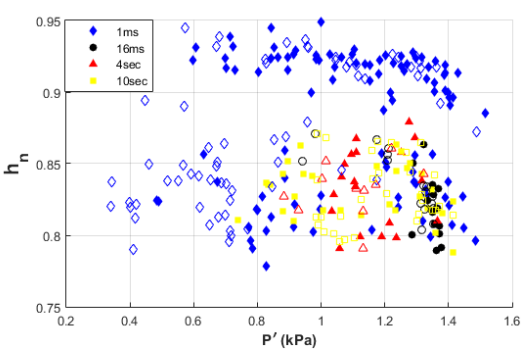

Figure 4: Permutation entropy against unstable pressure RMS for decay cases (filled markers) and rise cases (open markers) and transient durations.

In our previous work, we noticed roughly half of our tests experienced variable instability amplitudes. To separate the different behaviors, we binned each case into one of three categories based on its level of "apparent variation" during unstable combustion: low, medium, and high. Low apparent variation is characterized by a pressure signal with very little oscillation in the instability amplitude, as is shown in Figure 2(a). Medium apparent variation is when unstable combustion experiences one dip in combustion pressure no greater than one half of the overall unstable pressure, as in Figure 2(b). High apparent variation is characterized by a pressure signal that has more than one significant deviation in instability amplitude, as in Figure 2(c). There are 65 low, 51 medium, and 175 high variation cases considered in this paper.

An example of this categorization is shown in Figure 5, which plots the RMS of the normalized permutation entropy for both the stable and unstable portions of the signal for the low, medium, and high variation cases with a staging equivalence ratio of ϕ=0.8, rise cases only. We choose the staging equivalence ratio of ϕ=0.8 rise cases as these cases displayed the most variation of all the cases in the entire data set and so provide a clear example of the variation levels. These data are presented using box plots, which show the median (red line), the inner quartile range (IQR – blue boxes), and absolute maxima and minima (black whiskers) of the data so that we can identify statistically significant differences between cases. Outliers are defined as points outside the range of 1.5*IQR on either side of the median and are shown in red crosses.

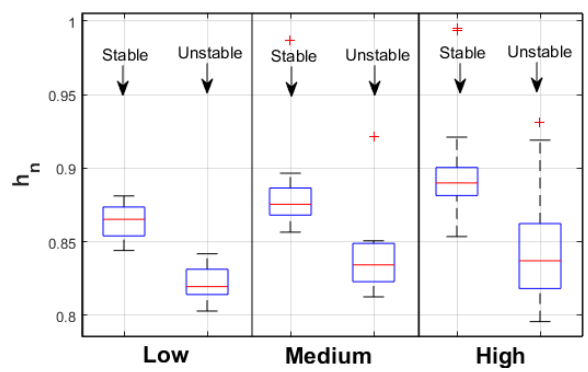

Figure 5. Permutation entropy for the three levels of variation and the stable and unstable portions of the pressure signal.

Figure 5 shows two important results. First, the normalized permutation entropy RMS is higher for the stable portion of the signal than the unstable portion. This result stems from the fact that the normalized permutation entropy is used and variations in the signal amplitude during the stable portion of the signal are large with respect to the mean. Second, there is an increasing trend in both the permutation entropy RMS as well as the spread of the permutation entropy as the variation level increases. These results show that the classification of the amplitude variation using the "apparent variation" criteria of low, medium, and high from visual inspection also aligns with the more quantitative analysis using the permutation entropy RMS.

Figure 6 shows the permutation entropy RMS as a function of transient timescale for the unstable, Figure 6(a), and stable, Figure 6(b), portions of the signal for all 291 cases. Both the permutation entropy RMS and the spread of the permutation entropy RMS are higher in the 1 ms cases than in every other case. These results show that the shortest time-scale cases show the most variability, likely because of the greatest disparity between the transient timescale and all other timescales in the system, particularly heat transfer timescales, as will be discussed later.

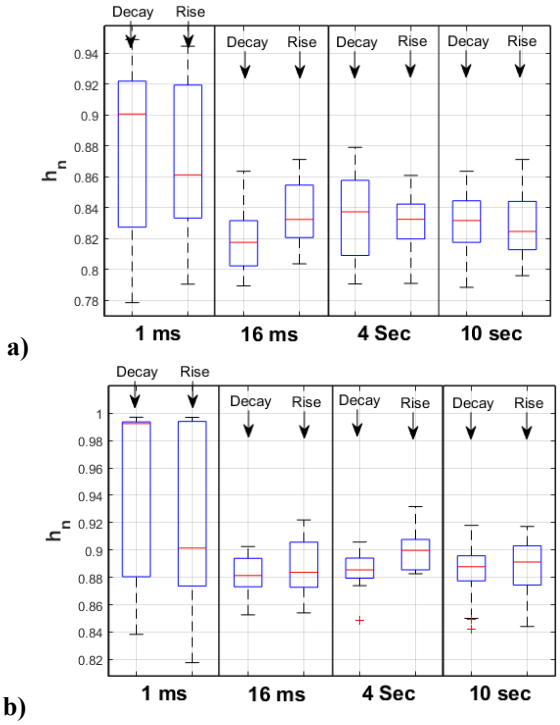

Figure 6. Permutation entropy RMS as a function of transient timescale and transient direction for a) unstable and b) stable portions of each test.

Further, there is no systematic difference between the permutation entropy RMS for rise and decay cases at any of the transient timescales, meaning that the variation does not display any hysteresis, despite the fact that the onset and decay processes were found to be quite different in previous studies [6]. In particular, for the same commanded transient timescale, the instability onset process typically took significantly longer than the instability decay process. Inspection of the instantaneous phase between the combustor pressure and the local heat release rate oscillations shows that during instability decay, the heat release rate and pressure oscillations gradually de-phase as the instability amplitude decreases. However, during instability onset, the heat release rate and pressure oscillations snap into phase despite a more gradual increase in the pressure oscillation amplitude. Despite these mechanistic differences in the instability onset and decay processes, the amplitude variation levels do not change.

Figure 7 shows the combustor growth rate during the unstable portion of the transient test for the low, medium, and high variation cases across all staging equivalence ratios, staging nozzles, and instability timescales. For decay cases, the unstable portion of the signal is the starting point of the transient, whereas for the rise cases, the unstable portion of the signal is after the transient has been conducted. Two interesting trends emerge from these results. First, the instability growth rate is significantly lower for the high variation cases than for the low, with the mid-level variation cases in the middle. This result shows the connection between variation and thermoacoustic growth rate in the system; the lower the growth rate, the more the signal amplitude varies in time. In these cases, the system is more susceptible to random fluctuations of the in-flow or boundary conditions that may change the instability amplitude.

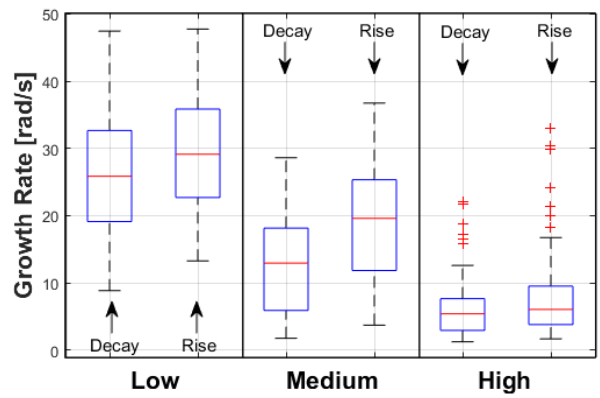

Figure 7. Combustor growth rate as a function of apparent intermittency and transient direction

Figure 7 also shows that rise cases have a slightly larger growth rate in each variation category, although the differences are only statistically significantly different in the mid-level variation cases as the median of the rise cases is above the inner quartile range of the decay cases. The same trend holds when separated out by staging nozzle, confirming that the staging nozzle does not have an effect on growth rate. These results are likely a result of the differences in thermal states before and after the transient, as will be described later.

Figure 8 shows the combustor damping rate during the stable portion of the transient operation for rise and decay cases in the three variation categories. These results show that the damping rate and the spread of the damping rate across all cases does not change for the three apparent variation cases. This is in contrast to the growth rate, shown in Figure 7, which is more strongly tied to the level of variation. As the damping rates are only calculated during the stable parts of the signal, this shows that the variation of the pressure amplitude in the stable portion of the signal is insensitive to the transient operation of the system regardless of whether it was before or after the transient event.

So far, we have shown that amplitude variation is connected to the thermoacoustic growth rate of the instability. Systems with low growth rates during the unstable portions of the signal can result in higher levels of variation in the pressure signal

amplitude. This result may point to a physical explanation for the variation in instability amplitude. Unlike previous studies by Nair et al. [12] that showed that the system intermittently jumps between stable and unstable states on either side of a Hopf bifurcation, the system during our analysis is either unstable or stable the entire time. Instead, the amplitude of the limit-cycle instability varies with time. This limit-cycle amplitude is determined by a balance between thermoacoustic driving and acoustic damping in the combustion system, and as these values fluctuate, the instability amplitude varies. Given the negative correlation between amplitude variation and instability growth rate, the results suggest that the amplitude variation occurs when the system is closer to the bifurcation point and is more sensitive to noise.

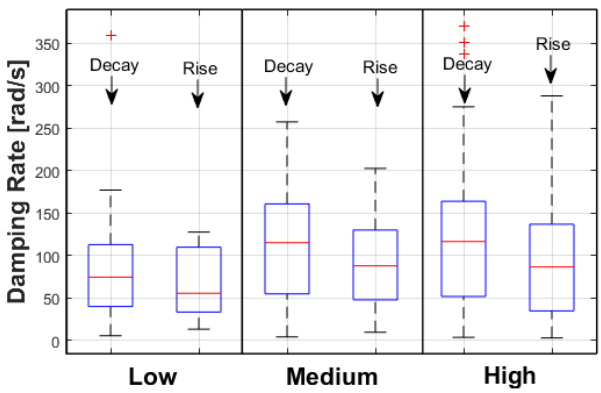

Figure 8. Combustor damping rate as a function of apparent intermittency and transient direction

The bifurcation point of this system was carefully characterized in previous work by Culler et al. [29], who defined a "bifurcation equivalence ratio," or the staging equivalence ratio at which each of the five nozzles resulted in instability suppression. For the center nozzle staging, which accounts for the vast majority of the data, the bifurcation equivalence ratio is ϕ=0.79; a resolution of 0.02 in equivalence ratio is repeatedly achievable with this experiment. As such, the operating conditions at ϕ=0.8, like those shown in Figure 5, where amplitude variation is found most often, are close to the bifurcation equivalence ratio and, as such, are more sensitive to noise in the system.

In correlating damping and growth rates with a large number of operational parameters, we found that combustor damping and growth rates most closely track centerbody temperature, which is representative of the thermal boundary condition at the stabilization point of the flame. Figure 9 shows centerbody temperature at the end of each test as a function of damping rate and growth rate for cases with a staging equivalence ratio of ϕ=0.8. The solid markers show decay cases and the open makers show the rise cases. We chose the final temperature as it is representative of the thermal condition over the course of the test; the initial temperatures were all maintained within a 10 °C range to ensure repeatability of each test and temperatures were not measured in the middle of the tests.

There are several important conclusions from Figure 9. Short transients have a lower final centerbody temperatures for both rise and decay cases than the long-duration cases. Work by this group and Bonciolini et al. [8] has shown that short-duration transient operation does not allow the thermal conditions at the wall to equilibrate over the course of the transient due to the high thermal inertia of the wall. In this way, the thermal boundary condition for the flame for short- and long-duration transients are different, which can have significant consequences for the stability of the flame.

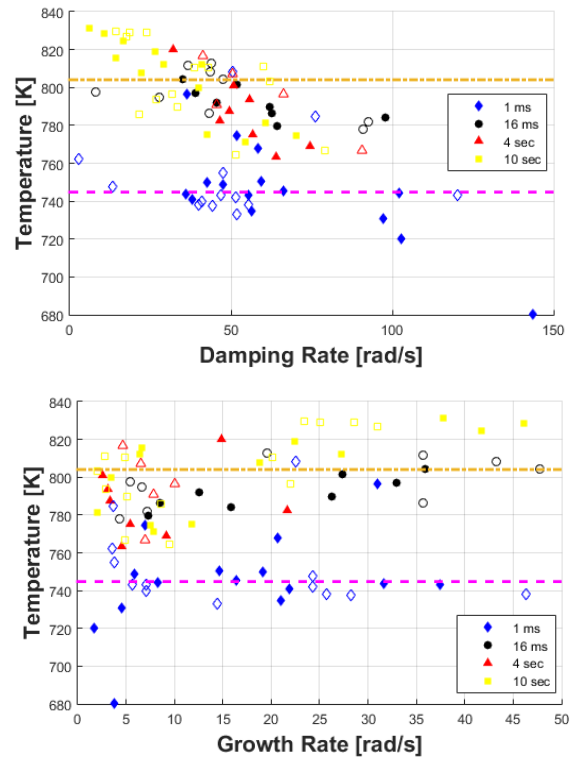

Figure 9. Final centerbody temperature against combustor a) damping rate and b) growth rate for staging equivalence ratio of 0.8 and instability rise (open markers) and decay (solid markers) cases.

These results also show that high centerbody temperatures are correlated with low damping rates during stable operation and high growth rates during unstable operation, indicating that thermoacoustic instability is stronger when the flame stabilization location is hotter. While this data does not indicate causation, work by Hong et al. [33] showed that combustion instability could be suppressed by using low thermal-conductivity materials at the flame-holding location in a backwards-facing step combustor; high thermal-conductivity materials with high temperatures at the flame-holding location lead to significantly higher instability amplitudes. This same trend is observed in this study, where operating conditions with high centerbody temperature have low damping rates and high growth rates, which result in lower levels of amplitude variation. The cases with colder centerbodies, which do not support strong instability, exhibit more variation in the instability amplitude.

The trends in damping and growth rate with centerbody temperature are particularly strong for the ϕ=0.8 staging equivalence ratio cases, but not as strong for the ϕ=0.85 or ϕ=0.9 cases. In these cases, the damping rate is higher overall due to the higher amplitude of staging [6]. In these cases, the instability is always suppressed and the system isn't operating close to a stability boundary, as it is in ϕ=0.8. While the impact of centerbody temperature is still measurable, it is not as strong as in the ϕ=0.8 cases.

Finally, the trends in thermoacoustic damping and growth rates with centerbody temperature are similar for both instability onset (open markers) and decay (solid markers) cases. This is another example of how the bulk parameters of the system are insensitive to transient direction, despite the flame processes occurring during the transition itself are significantly different for onset and decay cases, as discussed above. Despite the differences in the transition process, the beginning and end states scale similarly for these ranges of transient timescales.

CONCLUSION

This study investigated the underlying reasons for variation in the combustion instability amplitude over a range of operating conditions in a multi-nozzle combustor operated with transient fuel staging. A total of 291 test cases from over three years of research were categorized based on the variation in the pressure oscillation amplitude that occurred during both the stable and unstable portions of the signal. It was found that variation is larger in cases were thermoacoustic growth rate is lower and that lower growth rate is likely driven by the thermal boundary conditions at the flame attachment point, as has been seen in literature previously.

The results of this study have several important implications for future research and development of combustion systems, particularly in cases where transient operation may occur regularly. Capturing the thermal boundary condition of the flame, especially at its attachment point, is critical for understanding the instability amplitude. In simulation, conjugate modeling of combustion and surface heat transfer is necessary for predicting whether the system is unstable and what the instability amplitude might be. This thermal boundary condition can have a significant effect on the thermoacoustic growth rate, which impacts the final limit-cycle amplitude of the instability. Variation in the instability amplitude can be linked to the level of thermoacoustic growth and damping, where variation occurs in case with low damping (during stable operation) and low growth rates (during unstable operation). At these conditions, perturbations to the system are more likely to interrupt the thermoacoustic feedback processes, resulting in temporal fluctuations in the instability amplitude. Finally, permutation entropy RMS is a useful way of quantifying the variation of the signal during both the stable and unstable portions of combustor operation.

Future work will expand these ideas for possibly online prediction of combustion instability in complex combustion systems like the multi-nozzle combustor. Additionally, we will continue to analyze the instantaneous dynamics of the multi-nozzle combustor to understand the behavior of the system during transient operation. Previous experiments in the single-nozzle version of this combustor [34] showed far less instability amplitude variation and dependence on transient operating conditions. The many degrees of freedom that arise from operating a five-nozzle, highly turbulent combustion system result in richer dynamical behaviors, including issues related to amplitude variation. This experiment provides a unique opportunity to understand high-dimensional systems, like industrial gas turbine combustors, in a laboratory setting.

ACKNOWLEDGEMENTS

This work was funded by the US Department of Energy University Turbine Systems Research Program under grant DE-FE0025495 with program monitor Mark Freeman.

APPENDIX A: Permutation Entropy

Permutation entropy is a method to measure the complexity of time dependent data, as proposed by Bandt and Pompe [23]. Their method takes a series of points, x_i, of length l and ranks each sub-series, of length n, based on the occurrence of each value in the full time series. The permutation entropy of x_i is given by Eq. 3.

$$H_n = -\sum_{k=1}^{n!} p_k \log_2(p_k) \tag{3}$$

where p_k is the frequency of a permutation pattern occurring within x_i. The overall permutation entropy can range from 0 to $\log_2(n!)$. The normalized permutation entropy, h_n, is given by Eq. 4, which is Eq. 3 divided by $\log_2(n!)$.

$$h_n = \frac{H_n}{\log_2(n!)} \tag{4}$$

To understand the permutation entropy, we use an example from Riedl et al. [24]. Consider the time series $x = [6,9,11,12,8,13,5]$ with $n = 3$ and $\tau_{pe} = 1$. The first sub-series contains the values of x the order of [6,9,11], the next of [9,11,12], then [11,12,8] and so forth. Because $\tau_{pe} = 1$, each successive loop starts at $i + 1$. If $\tau_{pe} = 2$, then the first sub-series would include [6,9,11], the next [11,12,8], and the last sub-series would be [8,13,5] because it marks the end of the time series. By carefully selecting τ_{pe}, one can overlook the harmonic motion of a signal and single out the underlying complexity. The permutation entropy is then calculated by determining the frequency of a given pattern in each subseries.

REFERENCES

[1] Lieuwen, T. C., and Yang, V., 2005, Combustion instabilities in gas turbine engines: Operational experience, fundamental mechanisms and modeling, AIAA, Reston, VA.

[2] Rayleigh, 1878. "The Explanation of Certain Acoustical Phenomena". *Nature*, 18(4), pp. 319–321.

[3] Davis, L. B., and Black, S. H., 1995, "Dry Low NOx Combustion Systems for GE Heavy-Duty Gas Turbines," GE Power Systems, Schenectady, NY

[4] Samarasinghe, J., Culler, W., Quay, B. D., Santavicca, D. A., and O'Connor, J., 2017, "The Effect of Fuel Staging on the Structure and Instability Characteristics of Swirl-Stabilized Flames in a Lean Premixed Multi-Nozzle Can Combustor," ASME Turbo Expo

[5] Doleiden, D., Culler, W., Tyagi, A., Peluso, S., and O'Connor, J., 2019, "Flame Edge Dynamics and Interaction in a Multi-nozzle Can Combustor with Fuel Staging," *Journal of Engineering for Gas Turbines Power*, **141(**10). p. 101009

[6] Culler, W., Chen, X., Samarasinghe, J., Peluso, S., Santavicc, D. and O'Connor, J., 2018, "The Effect of Variable Fuel Staging Transients on Self-Excited Instabilities in a Multiple-Nozzle Combustor." *Combustion and Flame,* **194**, p. 472–484. DOI 10.1016/j.combustflame.2018.04.025.

[7] Culler, W., Samarasinghe, J., Quay, B., Santavicca, D. and O'Connor, J., 2017, "The Effect of Transient Fuel Staging on Self-Excited Instabilities in a Multi-Nozzle Model Gas Turbine Combustor," ASME Turbo Expo

[8] Bonciolini, G., Ebi, D., Doll, U., Weilenmann, M., and Noiray, N., 2019, "Effect of wall thermal inertia upon transient thermoacoustic dynamics of a swirl-stabilized flame." *Proceedings of the Combustion Institute,* **37**(4). p. 5351-5358. DOI 10.1016/j.proci.2018.06.229

[9] Boxx, I., Stohr, M., C. Carter, C. and Meier, W., 2010, "Temporally Resolved Planar Measurements of Transient Phenomena in a Partially Pre-Mixed Swirl Flame in a Gas Turbine Model Combustor." *Combustion and Flame,* **157**(8), p. 1510-1525. DOI 10.1016/j.combustflame.2009.12.015

[10] Steinberg, A., Boxx, I., Stohr, M. and Meier, W., 2012, "Effects of Flow Structure Dynamics on Thermoacoustic Instabilities in Swirl-Stabilized Combustion." *AAIA Journal,* **50**(4), p. 952-967. DOI 10.2514/1.J051466

[11] Steinberg, A., Boxx, I., Stohr, M. and Adrnt, C., 2011, "Influence of Flow-Structure Dynamics on Thermo-acoustic Instabilities in Oscillating Swirl Flames." AIAA/ASME/SAE/ASEE Joint Propulsion Conference and Exhibit

[12] Nair, V., Thampi, G. and Sujith, R., 2014, "Intermittency Route to Thermoacoustic Instability in Turbulent Combustors." *Journal of Fluid Mechanics* **756,** p. 470–487. DOI 10.1017/jfm.2014.468.

[13] Nair, V. and Sujith, R., 2015, "A Reduced-Order Model for the onset of Combustion Instability: Physical Mechanisms for Intermittency and Precursors." *Proceedings of the Combustion Institute,* **35**(3), p. 3193-3200. DOI 10.1016/j.proci.2014.07.007.

[14] Seshadri, A., Nair, V., and Sujith, R. I., 2016, "A Reduced-Order Deterministic Model Describing an Intermittency Route to Combustion Instability," *Combustion Theory and Modeling,* **20**(3), p. 441–456. DOI 10.1080/13647830.2016.1143123

[15] Bonciolini, G. and Noiray, N., 2019, "Bifurcation Dodge: Avoidance of a Thermoacoustic Instability Under Transient Operation" *Nonlinear Dynamics,* **96**, p. 703-716. DOI 10.1007/s11071-019-04815-y

[16] Lieuwen, T., 2005, "Online Combustor Stability Margin Assessment Using Dynamic Pressure Data," *Journal of Engineering for Gas Turbines Power*, **127**(3), p. 478–482. DOI 10.1115/1.1850493

[17] Stadlmair, N., Hummel, T. and Sattelmayer, T., 2018, "Thermoacoustic Damping Rate Determination from Combustion Noise Using Bayesian Statistics." *Journal of Engineering for Gas Turbines and Power*, **140**(11), p. 111501. DOI 10.1115/1.4038475

[18] Nair, V. and Sujith, R., 2013, "Identifying Homoclinic Orbits in the Dynamics of Intermittent Signals Through Recurrence Quantification." *Chaos,* **23**(3), p. 1 – 6. DOI 10.1063/1.4821475

[19] Juniper, M. P., and Sujith, R. I., 2018, "Sensitivity and Nonlinearity of Thermoacoustic Oscillations." *Annual Review of Fluid Mechanics*, **50**, p. 661-689. DOI 10.1146/annurev-fluid-122316-045125

[20] Kabiraj, L. and Sujith, R., 2012, "Nonlinear Self-Excited Thermoacoustic Oscillations: Intermittency and Flame Blowout." *Journal of Fluid Mechanics,* **713,** p. 376–397. DOI 10.1017/jfm.2012.463

[21] Unni, V., and Sujith, R., 2017, "Flame Dynamics during Intermittency in a Turbulent Combustor." *Proceedings of the Combustion Institute,* **36**(3), p. 3791–3798. DOI 10.1016/j.proci.2016.08.030.

[22] George, N., Unni, V., Raghunathan, M. and Sujith, R., 2018, "Pattern Formation during Transition from Combustion Noise to Thermoacoustic Instability via Intermittency." *Journal of Fluid Mechanics,* **849**, p. 615–644. DOI 10.1017/jfm.2018.427.

[23] Bandt, C. and Pompe, B., 2002 "Permutation Entropy: A Natural Complexity Measure for Time Series." *Physical Review Letters,* **88**(17), p. 174102. DOI 10.1103/PhysRevLett.88.174102.

[24] Riedl, M., Müller, A. and Wessel, N., 2013, "Practical Considerations of Permutation Entropy: A Tutorial Review." *European Physical Journal Special Topics,* **222**(2), p. 249–262. DOI 10.1140/epjst/e2013-01862-7.

[25] Sampath, R. and Chakravarthy, S., 2016, "Investigation of Intermittent Oscillations in a Premixed Dump Combustor using Time-Resolved Particle Image Velocimetry." *Combustion and Flame,* **172**, p. 309-325. DOI 10.1016/j.combustflame.2016.06.018.

[26] Murayama, S., Kinugawa, H., Tokuda, I. and Gotoda, H., 2018, "Characterization and Detection of Thermoacoustic Combustion Oscillations Based on Statistical Complexity and Complex-Network Theory." *Physical Review,* **97**(2), p. 022223. DOI: 10.1103/PhysRevE.97.022223.

[27] Wabel, T., Yang, S., Passarelli, M., Cirtwill, J., Saini, P., Venkatesan, K. and Steinberg, A., 2019, "Analysis of Transient Thermoacoustic Oscillations in a Liquid Fueled Gas Turbine Combustor at Elevated Pressures." AIAA Propulsion and Energy

[28] Samrasinghe, J., Peluso, S., Quay, B. and Santavicca, D., 2016, "The Three-Dimensional Structure of Swirl-Stabilized Flames in a Premixed Multinozzle Can Combustor." *Journal of Engineering for Gas Turbines and Power,* **138**(3), p. 031502. DOI 10.1115/1.4031439.

[29] Culler, W., Chen, X., Samarasinghe, J., Peluso, S., Santavicca, D., and O'Connor, J., 2018, "Comparison of Center Nozzle Staging to Outer Nozzle Staging in a Multi-Flame Combustor" ASME Turbo Expo

[30] Domen, S., Gotoda, H., Kuriyama, T., Okuno, Y, and Tachibana, S., 2015, "Detection and Prevention of Blowout in a Lean Premixed Gas Turbine Model Combustor Using the Concept of Dynamical System Theory." *Proceedings of the Combustion Institute,* **35**(3)**,** p. 3245 – 3253.

[31] Plummer, M. "JAGS Version 4.3.0 User Manual." (2015): pp. 0-41.

[32] Hummel, T., Berger, F., Stadlmair, N., Schuermans, B. and Sattelmayer, T., 2018, "Extraction of Linear Growth and Damping Rates of High-Frequency Thermoacoustic Oscillations from Time Domain Data," ASME Turbo Expo

[33] Hong, S., Shanbhogue, S., Kedia, K. and Ghoniem, A., 2013, "Impact of the Flame-Holder heat Transfer Characteristics on the Onset of Combustion Instability." *Combustion Science and Technology,* **185**(10), pp. 1541-1567. DOI 10.1080/00102202.2013.816575

[34] Chen, X., Culler, W., Peluso, S., Santavicca, D. and O'Connor, J. 2018, "Comparison of Equivalence Ratio Transients on Combustion Instability in a Single-Nozzle and Multi-Nozzle Combustors," ASME Turbo Expo